Article

Not peer-reviewed version

Color Rendering Index over 95 Achieved by Using Light Recycling Process Based on Hybrid Remote-type Red Quantum-dot Components Applied to Conventional LED Lighting Devices

Eunki Baek , Boseong Kim , Sohee Kim , Juyeon Song , Jaehyeong Yoo , Sung Min Park , Jong-Min Lee , Jae-Hyeon Ko *

Posted Date: 22 August 2023

doi: 10.20944/preprints202308.1484.v1

Keywords: quantum dot; LED; color rendering index; remote; quantum-dot component

Article

Color Rendering Index over 95 Achieved by Using Light Recycling Process Based on Hybrid Remote-Type Red Quantum-Dot Components Applied to Conventional LED Lighting Devices

Eunki Baek †, Boseong Kim †, Sohee Kim †, Juyeon Song †, Jaehyeong Yoo †, Sung Min Park, Jong-Min Lee and Jae-Hyeon Ko *

School of Semiconductor·Display Technology, Nano Convergence Technology Center, Hallym University, Chuncheon 24252, Gangwondo, Korea

* Correspondence: hwangko@hallym.ac.kr

† These authors contributed equally to this work.

Abstract: Red color conversion materials have often been used in conventional white LEDs (light-emitting diodes) to enhance the insufficient deep red component and thus improve the color rendering property. Quantum dots (QDs) are one of the candidates due to their flexibility in controlling the emission wavelength, which is attributed to the quantum confinement effect. Two types of remote QD components, i.e., QD films and QD caps, were prepared and applied to conventional white LED illumination to improve the color rendering properties. Thanks to the red component near 630 nm caused by the QD components, the color rendering indices(CRIs) of both Ra and R9 could be increased to over 95. It was found that both the diffusing nature of the reflector and the light recycling process in the vertical cavity between the bottom reflector and the top optical films play important roles in improving the color conversion efficiency of remote QD components. The present study showed that the proper application of remote QDs combined with a suitable optical cavity can control the correlated color temperature of the illumination over a wide range, thus realizing different color appearances of white LED illumination. In addition, a high CRI of over 95 could be achieved due to sufficient excitation from fewer QDs due to the strong optical cavity effect.

Keywords: quantum dot; LED; color rendering index; remote; quantum-dot component

1. Introduction

Lighting technology is undergoing a revolutionary change based on white LEDs (light-emitting diodes). A new way of producing white light could be realized by combining blue LED chips with color conversion materials such as phosphors [1]. The most typical color conversion material for white LEDs is Ce-doped yttrium aluminum garnet (YAG, $Y_3Al_5O_{12}$) [2], which is highly efficient and robust to environmental changes. However, it tends to lack a deep red component, which is the main reason for its low color rendering index (CRI) [3]. The color rendering properties of lighting are becoming increasingly important as people spend more time indoors following the outbreak of COVID-19. Several attempts have been made to improve the color rendering property of white LEDs, such as using the red and green phosphors simultaneously over the blue LEDs [4], applying red quantum dots (QDs) to the conventional LED lighting devices [5,6], etc.

QDs are promising color conversion materials due to their high purity, color tunability, and high quantum yield [7–9]. Due to their easy processibility and flexibility in the form factor, QDs have been adopted in the backlight for liquid crystal display (LCD) applications [10–16]. High color gamut has been achieved for LCD by using QD films in combination with blue LEDs due to the high color purities of the primary lights emitted by red and green QDs. In contrast, the use of QDs for general illumination has been less studied. One reason may be the vulnerability of QDs to high temperatures and other ambient conditions such as humidity and oxygen. In this context, the remote-type design can be used to improve the long-term stability of QD-based lighting devices. Recent studies show

 doi:10.20944/preprints202308.1484.v1

that the CRI can be significantly increased by using remote QD components in various forms [17–24]. QDs immersed in polymers or glass composites have been studied by many groups for the past decades [25–38]. The most successful commercialization of remote QD components is QD films in backlights for LCD applications. However, careful design of the optical structure is required when incorporating remote QD components into conventional lighting to improve color conversion efficiency and to avoid color dispersion [39]. Otherwise, color conversion efficiency may become low, or light reabsorption may reduce the lighting efficiency.

In our previous studies, either QD films or QD caps have been incorporated into conventional white LED lighting devices to improve color rendering properties [39–42]. Especially, the position of each QD component has been optimized by evaluating the optical characteristics of the white LEDs. However, the interaction between the remote QD structure and other optical components has not been systematically investigated. The performance of optical components or color conversion materials is affected by the optical structure in addition to the optical properties of the materials that make up the lighting devices. For example, the gain factor of reflective polarizers used to increase the brightness of LCDs is critically dependent on the optical properties of the backlights, such as the stack of optical films, the reflective properties of the lower part of the backlight, etc. [43,44]. It shows that the process of light recycling in optical devices, such as backlights and illumination devices, plays an important role in improving optical performance.

The purpose of this study is to investigate the optimal configuration of remote QD components, their interactions with other optical properties, and thus to optimize lighting devices to achieve the high color rendering characteristics of conventional white LEDs. In particular, hybrid QD lighting devices consisting of both QD films and QD caps have been incorporated into the optical structure. The position, number, and shape of the two QD remote components, the sequence of optical films, and the optical properties of the reflective surfaces have been optimized to achieve a high CRI of over 95.

2. Materials and Methods

A commercially available 6-inch, 15-W white LED lighting (KE15DN61S57A1, Partner Co., Gimpo, Korea) was adopted as a basic lighting fixture into which QD components were incorporated. Total 72 white LEDs with an emitting area of 3.2×2.8 mm^2 were arranged concentrically. Figure 1 shows the top-view of one of the adopted designs where the conventional white LED fixture can be seen together with remote QD components as described below. The upper and lower diameters of the lighting frame were 184 and 97 mm, respectively resulting in an inclination angle of the side reflector of 131.5°. The CRI and the correlated color temperature (CCT) of the original white LED device are 82.6 and 5626 K, respectively. The reflectance of the PCB (printed circuit board), on which white LEDs were arranges, was 69%. A polycarbonate (PC) diffuser with a diameter of 147 mm and a thickness of 2mm was used. The total transmittance and the haze of the diffuser were 69.9% and 99.2, respectively. The haze property was measured by using a haze meter (NDH-2000N, Nippon Denshoku, Tokyo, Japan).

Two remote red QD components were used; QD films and QD caps. Detailed fabrication process of the red QD films and QD caps have been reported before [39,41,42]. CdSe/ZnS core-shell QDs with an average diameter of ~6 nm were fabricated by using the conventional hot injection method. The emitting wavelength of the red QDs was ~623 nm. QD particles were mixed with irregular hollow silica (SG-HS40, Sukgyung At Co., Ansan, Korea) of a size of ~40±10 nm for dispersion. In order to fabricate QD films, the QDs were mixed with the triazine epoxy resin and coated on a PET (polyethylene terephthalate) substrate by using the roll-to-roll slot die method [39]. The QD concentration in the film was 7.5 wt%. At the initial stage, QD concentration of 5.0 wt% was also prepared and tested in the lighting. The QD caps (QD concentration of 5 wt%) of outer dimensions of 7.4×5.3×4.2 mm^3 and two lateral thicknesses of 0.9 and 1.8 mm were fabricated by using a UV curing agent (Miracle UV Resin) and red QDs according to the method described in Ref. 41. The upper surface has a rectangular opening with an area of 5.6×1.7 mm^2. Figure 1 shows a photograph showing the structure of the white LED. Some of the white LEDs were covered by QD caps, and the emitting

Preprints (www.preprints.org) | NOT PEER-REVIEWED | Posted: 22 August 2023 doi:10.20944/preprints202308.1484.v1

area was surrounded by the QD stripe. The grey circular component on the right side is the diffuser. The dimensions and the photograph of the used QD cap are also shown in the same figure. Figure S1 in the Supplementary Materials shows the optical components used in this study.

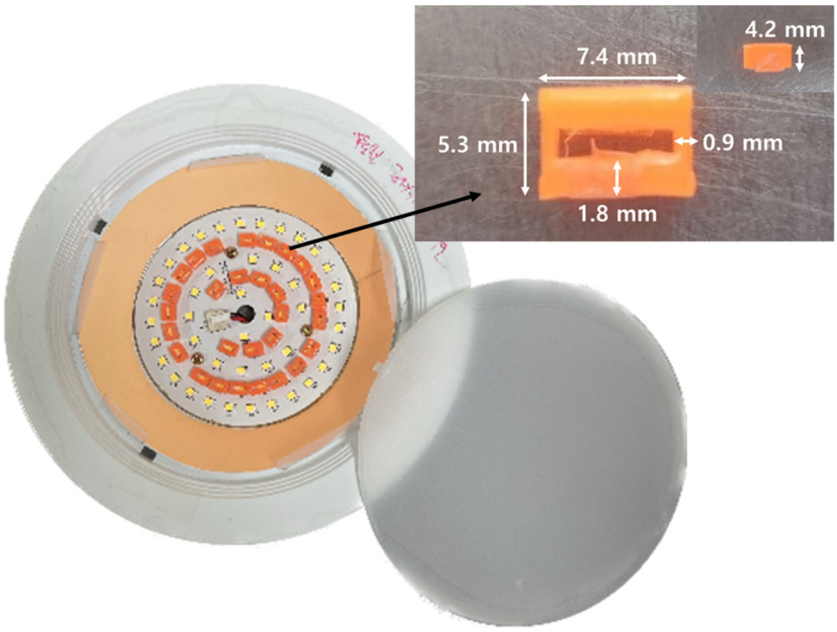

Figure 1. The photograph of a top-view of one of the adopted designs where the conventional white LED fixture can be seen together with remote QD components (the ring-type QD film and the QD caps). The detailed dimensions of the QD cap is also shown.

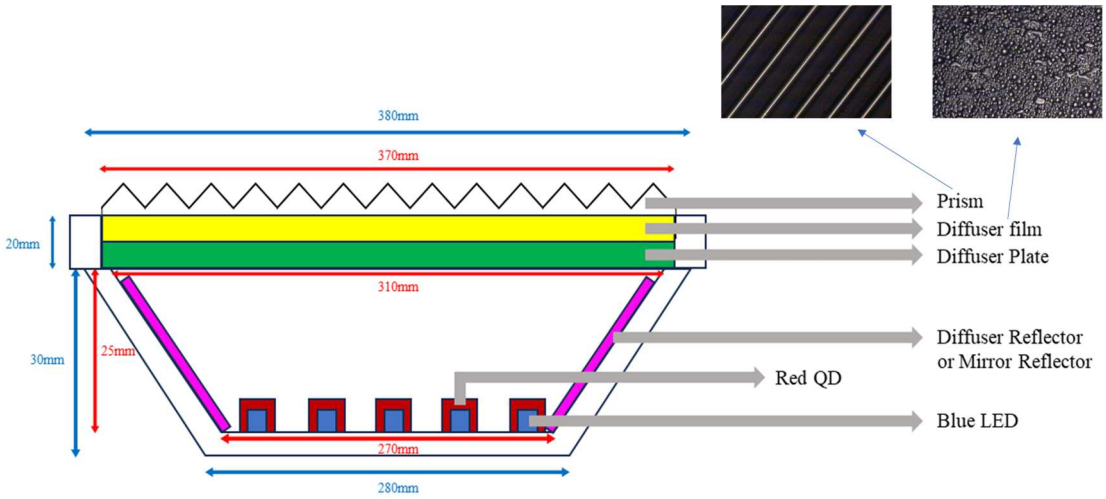

Figure 2. A cross-sectional view of the ring-type white LED lighting along with two microscopic photographs of the diffuser film and the prism film.

There were several factors in the optical configuration of the white LED: (1) the reflecting property of the reflector, whether the reflection is specular or diffuse, (2) whether the QD film was attached on the inclined side wall (which will be called "Ring-type") or set vertically (which will be called "Wall-type"), (3) the number of QD caps and their arrangement. The dimensions of the QD wall were 305×20 mm². The QD ring was designed to cover the inclined side wall as schematically shown in Figure S1(c). Figure 2 shows a cross-sectional view of the white LED. The top-view photographs of the diffuser film and the prism film are also shown in Figure 2. First, either a diffuse or a mirror reflector was laminated on the inclined side surface. The mirror reflector was an Al-coated one while the diffuse reflector was a typical white PET(Polyethylene terephthalate) film (See Figure

Preprints (www.preprints.org) | NOT PEER-REVIEWED | Posted: 22 August 2023 doi:10.20944/preprints202308.1484.v1

S1(a) and(b)). The ring-type and the wall-type QD films can ben seen from Figure S1(c) and (d), respectively. The 72 white LEDs were arranged in five concentric lines. Either the 12 white LEDs on the 3rd line or 29 white LEDs on the 2nd and 4th lines were covered by the red QD caps as shown in Figure S1(e) and (f). The on-axis luminance was recorded in terms of a 2D color analyzer (CA-2500A, Konica Minolta Co.). Table 1 shows several combinations of the optical films tried on the PC diffuser. Conventional optical films adopted in backlights, such as diffuser films and prism films, were used as shown in Figure 2. When two prim films were used, the directions of the prism grooves were perpendicular to each other.

The emitting spectrum, the color coordinates, the CRI, and the illuminance were measured by using an illuminance meter (CL-500A, Konica Minolta Co.). The distance between the center of the LED lighting and the color analyzer was 58 cm while that between the lighting and the illuminance meter was 32 cm. The average CRI can be divided into two, Ra and Re: The former is the average of R1 to R8, while the latter is the average of R1 to R15, including R9, which is associated with the deep red component.

Table 1. Dimensions and optical properties of the lighting frame and the PC diffuser plate.

Optical configuration	Abbreviation	Symbol
None (Only PC diffuser)	None	●
Diffuser film	D	■
Diffuser film + one prism film	D+P1	◆
Diffuser film + two prism films	D+P2	▲
One prism film	P1	▼
Two prism films	P2	◂

3. Results and Discussion

As a first step, the wall-type LED lighting without any QD caps was investigated for two QD concentrations, 5 and 7.5 wt%, and two reflector types. Figure S2(a) shows the dependence of the correlated color temperature (CCT) of the LED lighting on the reflector property and the QD concentration. As the QD concentration increases from5 to 7.5 wt%, the CCT decreases due to the larger color conversion efficiency. On the other hand, the CCT decreases when the reflector is changed from the mirror-type to the diffuse-type. In the case of diffuse reflector, the reflected light is directed toward many different directions in the light cavity formed by the bottom and side reflectors and the top PC diffuser. Diffusely reflected light is expected to pass through the QD wall more times than the case of mirror reflector. The enhanced color conversion at the higher QD concentration under the condition of the diffuser reflector increases the CRI as shown in Figure S2(b). Thus, We will focus on the two conditions, i.e., at the QD concentration of 7.5 wt% and the diffuser reflector henceforth. The results obtained from the LED lighting with a mirror reflector will be compared if necessary.

Total 12 designs were investigated depending on the reflector type, the configuration of the QD film (wall-type and ring-type), and the arrangement of the QD caps. Table S1 in the Supplementary Materials shows the categories of the 12 designs together with the corresponding photos. “Hybrid 1~4” configurations denote the cases where no QD caps were used. “Hybrid 5~8” configurations are associated with the cases where 12 QD caps were adopted as shown in Figure S1(e). “Hybrid 9~12” configurations are related to the cases where 29 QD caps were arranged according to Figure S1(f).

Figures S3(a)~(d) in the Supplementary Materials summarizes the results obtained from the “Hybrid 1~4” configurations. The luminance values are nearly the same within 1%. However, the CCT of the ring-type configuration with a mirror reflector show the highest CCT compared to other configurations (See Figure S3(b)). In this case, the light hitting the QD ring on the mirror reflector is

Preprints (www.preprints.org) | NOT PEER-REVIEWED | Posted: 22 August 2023 doi:10.20944/preprints202308.1484.v1

reflected from the tilted mirror reflector surface in the normal direction without further conversion. On the other hand, the diffuse reflector under the QD ring can redirect light in different directions and increase the chance of further color conversion, resulting in a lower CCT value. The thin QD layer of the QD wall is formed on the transparent PET film so that the randomly directed light is more likely to be converted by the QD wall, resulting in a lower CCT. This enhanced color conversion is responsible for the higher CRI values of the wall-configuration with a diffuse reflector, as shown in Figure S3(c)~(d).

Figure 3 shows the results obtained from the "Hybrid 5~8" configurations where 12 QD caps were applied. The overall luminance values become lower when QD caps are used in LED lighting due to the conversion of the green component to the red component, which is less sensitive to the human eye. Luminance is highest for the Hybrid-8 configuration, where color conversion is expected to be highest due to the diffuse reflective property of the reflector and the wall-type configuration that intersects the light trapped in the lighting cavity. This is supported by the lowest CCT shown in Figure 3(b). The improved color conversion via the QD caps increases the Ra above 90 in all configurations, especially in the cases where the diffuse reflector is used (See Figure 3(c) and (d)). This may be due to the diffusely propagating light in the cavity resulting in more enhanced color conversion efficiency of QD components.

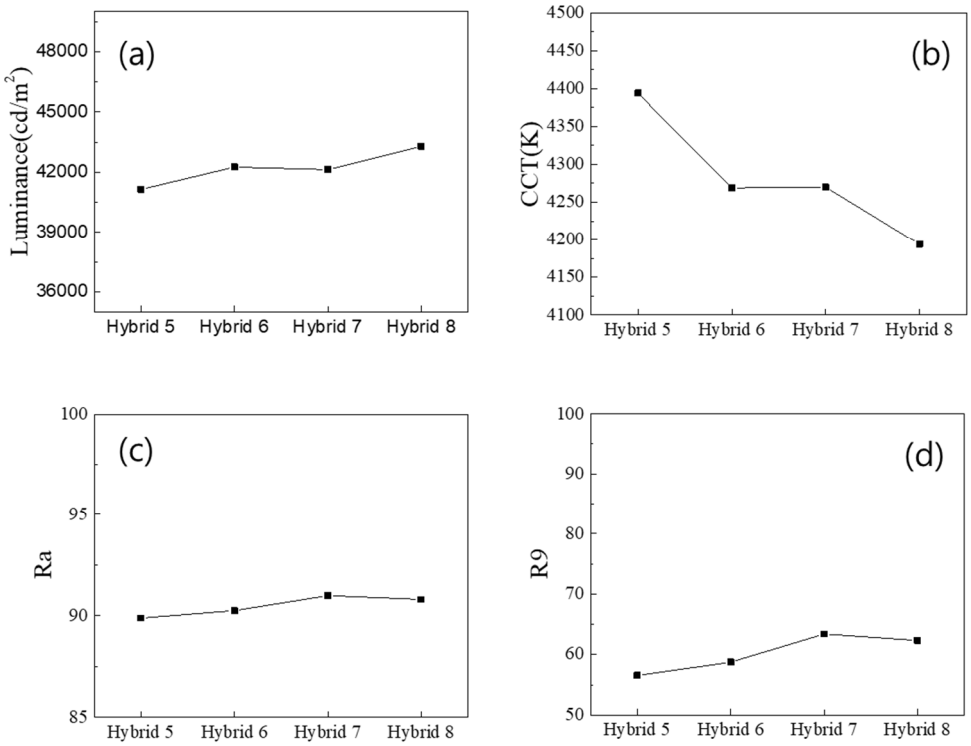

Figure 3. Photometric and color properties of the "Hybrid 5~8" configurations: (a) the luminance, (b) the CCT, (c) the Ra, and (d) the R9 CRI values.

These trends are more pronounced in the "Hybrid 9~12" configurations, where 29 QD caps were used, as shown in Figure 4. These results indicate that using the diffuse reflector is a better choice for increasing the color conversion efficiency of the remote QD component, and that the wall-type configuration is better for higher CRI values than the ring-type configuration. In particular, the Hybrid 11~12 configurations had Ra values above 95, which is highly desirable for high color rendering applications.

Preprints (www.preprints.org) | NOT PEER-REVIEWED | Posted: 22 August 2023 doi:10.20944/preprints202308.1484.v1

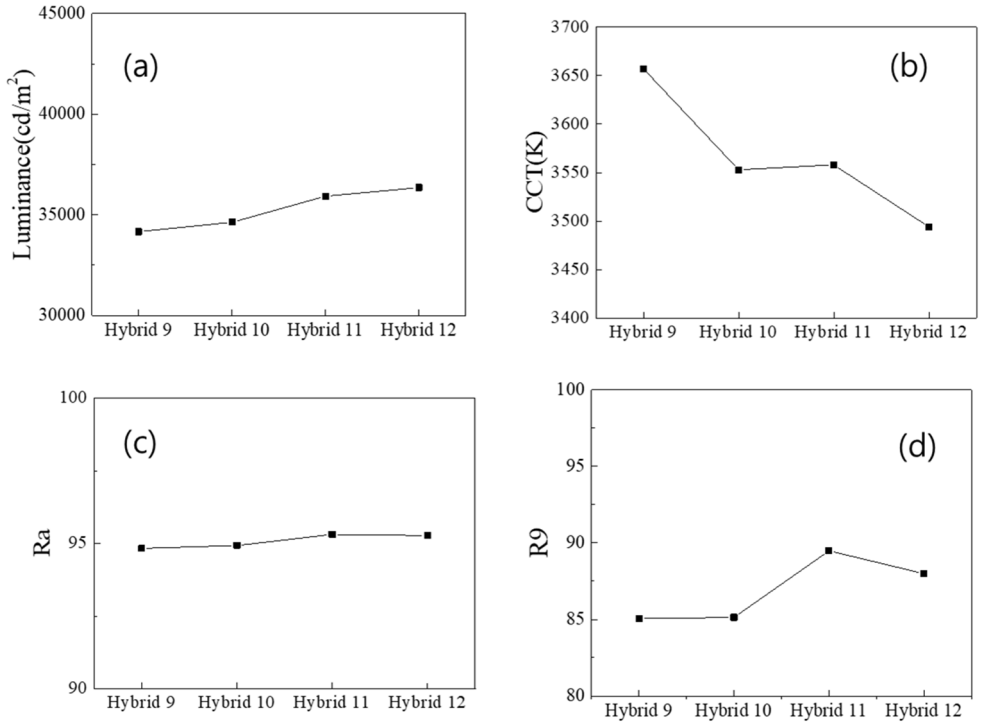

Figure 4. Photometric and color properties of the "Hybrid 9~12" configurations: (a) the luminance, (b) the CCT, (c) the Ra, and (d) the R9 CRI values.

The results from the Hybrid 5-12 configurations clearly show that the diffuse reflector with QD caps is more favorable for achieving high luminance. Instead of being redirected and escaping along the normal direction by the mirror reflector, the diffuse reflector tends to scatter the light in the cavity and increase the color conversion efficiency via the QD caps/films, resulting in higher luminance. In addition, when the luminance increases, the CCT tends to decrease, and the CRI tends to increase. This is mainly due to the fact that when the red component in the spectrum is increased via the red QD films or caps, the color rendering property is improved, resulting in lower CCT and higher CRI values. Therefore, from the point of view of color rendering properties, the Hybrid 11~12 configurations are the most favorable. Figures S4(a) and (b) in the Supplementary Materials show all the individual CRI values of the white LED illumination without any QD components and that with 29 QD caps together with the ring configuration (Hybrid 11 configuration), respectively. All CRI values increased significantly, especially the R9 associated with the deep red component as the Hybrid 11 configuration was adopted in the white LED lighting. Thanks to the improvement of R9, the extended CRI Re could reach ~94, as shown in Figure S4(b).

In the next step, different combinations of optical films shown in Table 1 were applied to the top of the PC diffuser to study the effect of the light recycling in the cavity on the optical properties. It is well known that some of the light incident on the microlens arrays is reflected back. For example, about half of the incident light is reflected back from the microprism grooves of the prism film. This type of light recycling plays an important role in improving the luminance of the backlight for LCD applications [43,44]. Figures 5(a) and (b) show two examples of the emitting spectra of the white LED illumination of the "Hybrid 3" (no QD caps and a ring-type QD film) and "Hybrid 11" configurations (29 QD caps and a ring-type QD film), respectively, under six different combinations of optical films on the PC diffuser. The relative intensity of the red peak near 630 nm, which represents the color conversion efficiency of the QD components, changes drastically depending on the combination of optical films.

Preprints (www.preprints.org) | NOT PEER-REVIEWED | Posted: 22 August 2023 doi:10.20944/preprints202308.1484.v1

When there is no QD cap, the peak near 630 nm shown in Figure 5(a) represents the color conversion efficiency of the ring-type QD film. If there is no optical film other than the PC diffuser, the QD film is rarely excited. The QD film is more excited when additional optical films are placed on the PC diffuser because a portion of the light incident on the film is reflected downward and contributes to the excitation of the ring-type QD film. In particular, the QD film is most excited when two prism films are placed on the PC diffuser due to the light recycling capability. A large portion of the light travels back and forth between the prism grooves and the bottom reflector, contributing to the excitation of the QD film. Figures S5(a)~(d) in the Supplementary Materials show the luminance, the CCT, the Ra, and the R9, respectively, of "Hybrid 1~4" configurations depending on the combination of optical films placed on the PC diffuser. The CCT decreases with a sequence of D → P1 → D-P1 → P2 → D-P2 according to the excitation level of the QD film in the cavity regardless of the configuration. Along the same sequence, the CRI values increase due to more excitation of the red component. However, the difference in the CRI values between the P2 and the D-P2 cases are very small.

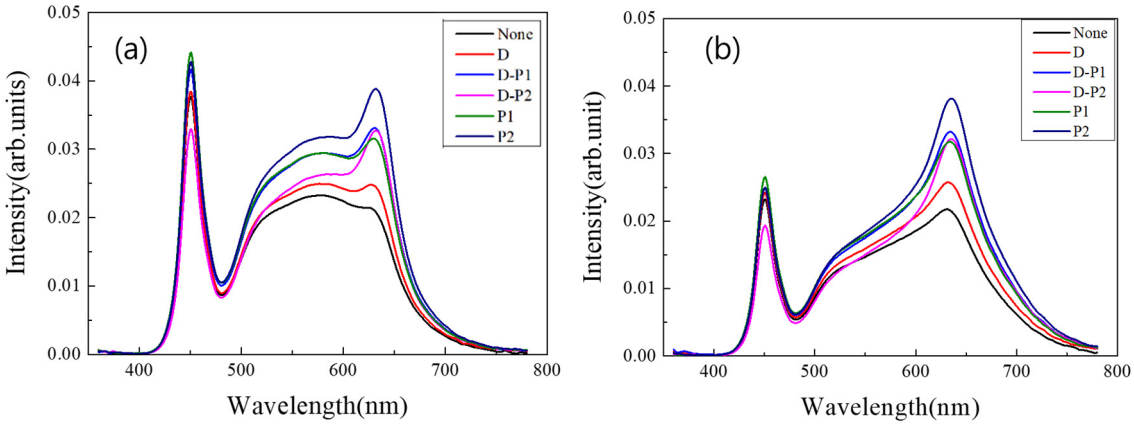

Figure 5. Emitting spectra of (a) the Hybrid 3 configuration and (b) the Hybrid 11 configuration under six different combinations of optical films.

Figure S6(a)~(d) in the Supplementary Materials show the luminance, the CCT, the Ra, and the R9, respectively, of "Hybrid 5~8" configurations depending on the combination of optical films placed on the PC diffuser. The general trend is similar to the case of "Hybrid 1~4" configurations shown in Figure S5. It should be noted that the CRI values increase significantly as the light recycling effect becomes more pronounced under two prism films. The R9 reached values greater than 94, and thus the Ra became ~96 under two prism films in the Hybrid 7 configuration (diffuse reflector, 12 QD caps, and the ring-type QD film). The CCT could be adjusted in a wide range between 4200 and 3350 K as shown in Figure S6(b). It demonstrates that colorimetric properties can be controlled over a wide range by appropriately combining remote QD components and optical films.

Figure 5(b) shows that the blue and green components of the spectrum are significantly reduced when 29 QD caps are included in the illumination due to further excitation of the QD materials in the caps. This trend becomes more pronounced when optical films are placed on the PC diffuser, especially when two prism films are combined and placed on the diffuser. Figure 6(a)~(d) show the luminance, the CCT, the Ra, and the R9, respectively, of "Hybrid 9~12" configurations depending on the combination of optical films placed on the PC diffuser. Figure S7 in the Supplementary Materials shows the same data, but, only for the "Hybrid 11" configuration as one representative example. Luminance is maximized when two prismatic films are placed on the PC diffuser due to their collimating functions. In this case, the viewing angle becomes narrower and the white LED lighting illuminates a smaller area at a higher intensity. Due to the much higher color conversion efficiency of the light recycling process, the CCT was lowered to ~2800 K, as shown in Figure 6(b), which is a very warm yellowish light. As shown in Figure 6(c), Ra does not improve significantly for the "Hybrid 9~12" configurations, even under the optical films. These configurations already have high enough

Preprints (www.preprints.org) | NOT PEER-REVIEWED | Posted: 22 August 2023 doi:10.20944/preprints202308.1484.v1

CRI values above 95. Optical films enhance the red component more, thus disturbing the spectral balance over the visible range, resulting in lower Ra. However, the enhancement of the red component by optical films definitely increases the R9 above 97 for some configurations, as can be seen in Figure 6(d).

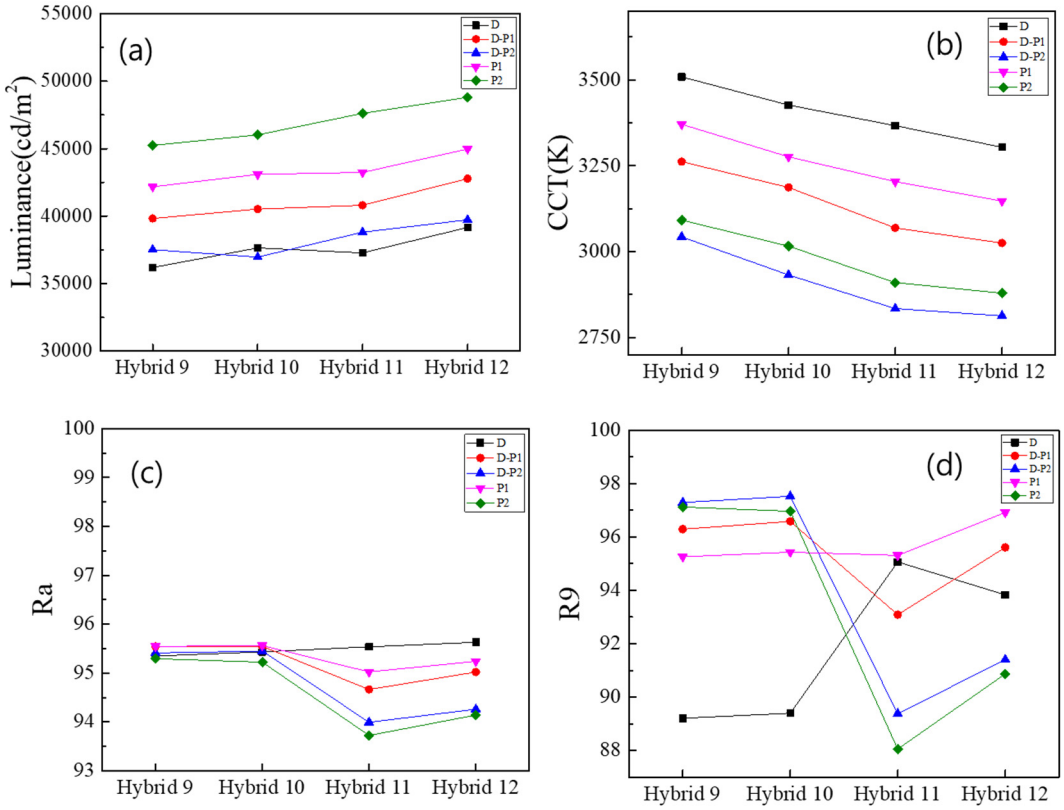

Figure 6. (a) The luminance, (b) the CCT, (c) the Ra, and (d) the R9 of "Hybrid 9~12" configurations depending on the combination of optical films placed on the PC diffuser.

Figure 7(a)-(c) show the chromaticity diagram showing the changes in color coordinates depending on the optical film combinations for the Hybrid 3, 7, and 11 configurations, respectively. These configurations are characterized by the diffuser reflector and the ring-type QD film. The color coordinates shift to the red region as the number of QD caps increases. In the same configuration, the color coordinates shift to the red region as the number of optical films increases, especially when two prism films are used. The color coordinates of the white LED with the "Hybrid 3" configuration nearly coincide with the Planckian locus. However, the difference in color coordinates between the ideal Planckian locus and the experimental points increases with the number of QD caps. This is mainly due to the increased red component caused by the QD caps, which pushes the color coordinates to the right lower part of the chromaticity diagram. As shown in Figure 7, the proper application of remote QD components can control the color coordinates in a wide range, thus realizing different color appearance of white LED illumination.

 doi:10.20944/preprints202308.1484.v1

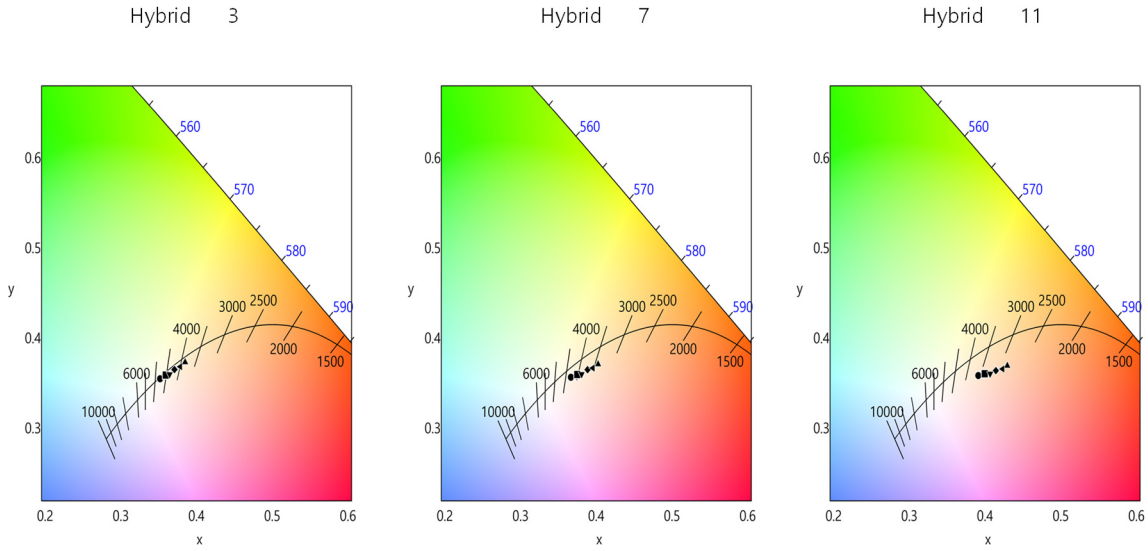

Figure 7. The chromaticity diagram showing the changes in color coordinates depending on the optical film combinations for the Hybrid 3, 7, and 11 configuration from left to right.

4. Conclusion

Two remote red QD components, i.e. QD films and QD caps, have been applied to conventional high-power white LED lighting to improve its color rendering performance. A total of 12 different configurations with six different combinations of optical films were investigated to find the optimum optical structure. Several design rules can be derived from this systematic investigation.

First, the application of red QDs is an effective way to enhance the red spectral component and thus improve the color rendering performance of conventional white LEDs. The ring-type or wall-type QD film can be used to achieve Ra over 87. Using the combination of both QD films and QD caps, it was possible to achieve both Ra and R9 above 95.

Second, using the diffuse reflector was more favorable for achieving high color rendering performance than using the mirror reflector. The diffuse reflector redirects the reflected light in different directions within the cavity, improving the color conversion efficiency of the red QDs. Thanks to this effect, the CCT was reduced and the CRI values increased with the adoption of the diffuse reflector.

Finally, constructing a strong vertical cavity between the bottom reflector and the top of the LED lighting is an efficient way to improve the color conversion efficiency of red QD components. As the number of optical films increased or two prism films were used, the intensity of the red peak near 630 nm was greatly increased. To adopt optical film to improve the color rendering performance was more effective for the configurations where fewer number of QD components was used. If the CRI is already high enough, it is not possible to improve it further by using optical films, because a strong cavity enhances the red component excessively and thus disturbs the spectral balance in the visible range, resulting in a lower Ra.

The present study showed that proper application of remote QD components combined with appropriate optical cavity can control the color coordinates of illumination in a wide range, thus realizing different color appearance of white LED illumination. In addition, a high CRI of over 95 could be achieved due to sufficient red excitation from fewer QD components and strong optical cavity effect.

Author Contributions: J.-H.K., J.-M.L. and S.M.P. conceived and designed the research; E.B., B.K., S.K., J.S., and J.Y. performed the simulation and experiments; E.B., B.K., S.K., J.S., J.Y, S.M.P., J.-M.L. and J.-H.K. carried out a formal analysis of the experimental data; J.-H.K.prepared the original draft; E.B., B.K., S.K., J.S., J.Y, S.M.P., J.-M.L. and J.-H.K. reviewed and did editing. All authors have read and agreed to the published version of the manuscript.

Funding: This work was supported by the National Research Foundation of Korea(NRF) grant funded by the Korea government(MSIT) (No. RS-2023-00219703).

Acknowledgment: The authors thank GLVISION Co. and Cheorwon Plasma Research Institute for helping us with preparing the QD components.

Conflict of Interest and other Ethics Statements: The authors declare no conflict of interest. The submitting author declares that: (i) the manuscript, or part of it, neither has been published nor is currently under consideration for publication by any other journal and that (ii) its publication is approved by all authors and tacitly or explicitly by the responsible authorities where the work was carried out, and that, if accepted, it will not be published elsewhere in the same form, in English or in any other language, without the written consent of the copyright-holder.

References

1. E. F. Schubert, J. K. Kim, H. Luo, J. -Q. Xi, *Rep. Prog. Phys.* **2006**, 69, 3069.
2. J. McKittrick, L. E. Shea-Rohwer, *J. Am. Ceram. Soc.* **2014**, 97, 1327.
3. T. Erdem, H. V. Demir, *Nanophotonics* **2013**, 2, 57.
4. H. -W. Choi, M. H. Choi, J. -H. Ko, *New Phys.: Sae Mulli* **2013**, 63, 1149.
5. K. A. Denault, A. A. Mikhailovsky, S. Brinkley, S. P. DenBaars, R. Seshadri, *J. Mater. Chem. C* **2013**, 1, 1461.
6. S. -R. Chung, S. -S. Chen, K. -W. Wang, C. -B. Siao, *RSC Adv.* **2016**, 6, 51989.
7. W. K. Bae, J. Lim, D. Lee, M. Park, H. Lee, J. Kwak, K. Char, C. Lee, S. Lee, *Adv. Mater.* **2014**, 26, 6387.
8. S. J. Lim, M. U. Zahid, P. Le, L. Ma, D. Entenberg, A. S. Harney, J. Condeelis, A. M. Smith, *Nat. Commun.* **2015**, 6, 8210.
9. J. Lim, Y. S. Park, K. Wu, H. J. Yun, V. I. Klimov, *Nano Lett.* **2018**, 18, 6645.
10. D. Bera, L. Qian, T. -K. Tseng, P. H. Holloway, *Materials* **2010**, 3, 2260.
11. H. V. Demir, S. Nizamoglu, T. Erdem, E. Mutlugunand, N. Gaponik, Alexander Eychmüller, *Nano Today* **2011**, 6, 632.
12. M. J. Anc, N. L. Pickett, N. C. Gresty, J. A. Harris and K. C. Mishra, *ECS J. Solid State Sci. Technol.* **2012**, 2, R3071.
13. Z. Luo, Y. Chen, S. -T. Wu, *Opt. Express* **2013**, 21, 26269.
14. E. Jang, S. Jun, H. Jang, J. Lim, B. Kim, Y. Kim, *Adv. Mater.* **2010**, 22, 3076.
15. S. Abe, J. J. Joos, L. IDJ Martin, Z. Hens, P. F. Smet, *Light Sci. Appl.* **2017**, 6, e16271.
16. S. J. Kim, H. W. Jang, J. -G. Lee, J. -H. Ko, Y. W. Ko, Y. Kim, *New Phys.: Sae Mulli* **2019**, 69, 861.
17. J. -Y. Lien, C. -J. Chen, R. -K. Chiang, S. -L. Wang, *Opt. Express* **2016**, 24, A1021.
18. J. -H. Kim, D. -Y. Jo, K. -H. Lee, E. -P. Jang, C. -Y. Han, J.-H. Jo, H. Yang, *Adv. Mater.* **2016**, 28, 5093.
19. H. C. Yoon, J. H. Oh, S. Lee, J. B. Park, Y. R. Do, *Sci. Rep.* **2017**, 7, 2808.
20. J. -H. Kim, B. -Y. Kim, E. -P. Jang, C. -Y. Han and J. -H. Jo, Y. R Do, H. Yang, *J. Mater. Chem. C* **2017**, 5, 6755.
21. H. Zhang, Q. Su, S. Chen, *Nat. Commun.* **2020**, 11, 2826.
22. S. Rhee, K. Kim, J. Roh, J. Kwak, *Curr. Opt. Photon.* **2020**, 4, 161.
23. B. Li, M. Lu, J. Feng, J. Zhang, P. M. Smowton, J. I. Sohn, I.-K. Park, H. Zhong, B. Hou, *J. Mater. Chem. C* **2020**, 8, 10676.
24. A. Hong, J. Kim, J. Kwak, *Adv. Opt. Mater.* **2020**, 8, 2001051.
25. J. Lee, V. C. Sundar, J. R. Heine, M. G. Bawendi, and K. F. Jensen, *Adv. Mater.* **2000**, 12, 1102.
26. H. Zhang, Z. Cui, Y. Wang, K. Zhang, X. Ji, C. Lü, B. Yang, and M. Gao, *Adv. Mater.* **2003**, 15, 777.
27. C. Li, and N. Murase, *Langmuir* **2004**, 20, 1.
28. C. Bullen, P. Mulvaney, C. Sada, M. Ferrari, A. Chiasera, and A. Martucci, *J. Mater. Chem.* **2004**, 14, 1112.
29. Q. Wang, N. Iancu, and D.-K. Seo, *Chem. Mater.* **2005**, 17, 4762.
30. M. C. Neves, M. A. Martins, P. C. R. Soares-Santos, P. Rauwel, R. A. S. Ferreira, T. Monteiro, L. D. Carlos, and T. Trindade, *Nanotech.* **2008**, 19, 155601.
31. H. Tetsuya, T. Ebina, and F. Mizukami, *Adv. Mater.* **2008**, 20, 3039.
32. E. Mutlugun, P. L. Hernandez-Martinez, C. Eroglu, Y. Coskun, T. Erdem, V. K. Sharma, E. Unal, S. K. Panda, S. G. Hickey, N. Gaponik, A. Eychmüller, and H. V. Demir, *Nano Lett.* **2012**, 12, 3986.
33. S. Jun, J. Lee, and E. Jang, *ACS Nano* **2013**, 7, 1472.
34. J.-H. Kim, and H. Yang, *Nanotech.* **2014**, 25, 255601.
35. S.-H. Lee, K.-H. Lee, J.-H. Jo, B. Park, Y. Kwon, H. S. Jang, and H. Yang, *Opt. Mater. Exp.* **2014**, 4, 1297.
36. Y. Altintas, S. Genc, M. Y. Talpur, and E. Mutlugun, *Nanotech.* **2016**, 27, 295604.
37. S. Yu, B. Fritz, S. Johnsen, D. Busko, B. S. Richards, M. Hippler, G. Wiegand, Y. Tang, Z. Li, U. Lemmer, H. Hölscher, and G. Gomard, *Adv. Opt. Mater.* **2019**, 7, 1900223.
38. G. Y. Kim, S. Kim, J. Choi, M. Kim, H. Lim, T. W. Nam, W. Choi, E. N. Cho, H. J. Han, C. Lee, J. C. Kim, H. Y. Jeong, S.-Y. Choi, M. S. Jang, D. Y. Jeon, and Y. S. Jung, *Nano Lett.* **2019**, 19, 6827.

39. S. C. Hong, S. T. Gwak, S. Park, G. J. Lee, J.-G. Lee, J.-H. Ko, S. Y. Joe, Y. Kim, T. Park, and Y. W. Ko, *Curr. Appl. Phys.* **2021**, 31, 199.
40. J.-G. Lee, G. J. Lee, S. C. Hong, J.-H. Ko, T. Park, and Y. W. Ko, *J. Korean Phys. Soc.* **2021**, 78, 822.
41. G. J. Lee, S. C. Hong, J.-G. Lee, J.-H. Ko, T. Park, Y. W. Ko, and S. Lushnikov, *Nanomaterials* **2022**, 12, 1097.
42. S. C. Hong, and J.-H. Ko, *Nanomaterials* **2022**, 12, 2864.
43. S. H. Jeong, A. Park, S. J. Kim, D. J. Park, and J.-H. Ko, *New Phys.: Sae Mulli* **2019**, 69, 101.
44. J. S. Seo, T. E. Yeon, and J.-H. Ko, *J. Opt. Soc. Korea* **2012**, 16, 151.